Effects of tryptophan mutation on the deprotonation and reprotonation kinetics of the Schiff base during the photocycle of bacteriorhodopsin

Shuguang Wu,* Yuejin Chang,* M. A. El-Sayed,* Thomas Marti,‡ Tatsushi Mogi,‡ and H. Gobind Khorana‡

*Department of Chemistry and Biochemistry, University of California-Los Angeles, Los Angeles, California 90024 USA; and
‡Department of Chemistry and Biology, Massachusetts Institute of Technology, Cambridge, Massachusetts 02139 USA

ABSTRACT The rates of deprotonation and reprotonation of the protonated Schiff base (PSB) are determined during the photocycle of nine bacteriorhodopsin mutants in which Trp-10, 12, 80, 86, 137, 138, 182 and 189 are individually substituted by either phenylalanine or cysteine. Of all the mutants, the replacement of Trp-86, Trp-182, and Trp-189 by phenylalanine and Trp-137 by cysteine is found to significantly alter the rate of the deprotonation, but not that of the reprotonation process. As compared with ebR, the Trp-86 mutation dramatically increases the rate of deprotonation of the PSB while the Trp-182 mutation greatly decreases this rate. Temperature dependence studies on the rate constants of the deprotonation demonstrate that the different energetic and entropic effects of the mutation are responsible for the observed different kinetic behavior of the Trp-86 and Trp-182 mutants as compared with that of ebR. In the case of Trp-86 mutant, a large decrease in both energy and entropy of activation suggests that the mutation of this tryptophan residue opens up the protein structure as a result of eliminating the hydrogen-bonding group on its side chain by a phenylalanine substitution.

A correlation is observed between the proton pumping yield and the relative amplitudes of the slow deprotonation component but not with rate constants of the rise or decay process at constant pH. These results are best discussed in terms of the heterogeneity model (with parallel cycle) rather than back reaction model.

INTRODUCTION

Bacteriorhodopsin (bR) functions as a light-driven proton pump and converts light into chemical energy by pumping protons across the bacterial membrane (1). Upon absorption of light, the light adapted bR undergoes a photocycle that involves a number of spectroscopically distinct intermediates: $bR_{560} \rightarrow K_{610} \rightarrow L_{550} \rightarrow M_{412} \rightarrow N_{520} \rightarrow O_{640} \rightarrow bR_{560}$.

bR contains 8 tryptophan residues out of a total 248 amino acid residues in its polypeptide chain (2). The possible involvement of tryptophan residues in bR proton pumping has been studied by several different techniques (3–8). Fluorescence quenching upon retinal binding revealed that most of tryptophans in bR interact with the retinal chromophore (4–6). A time-resolved fluorescence study has detected the photolysis-induced changes in the fluorescence intensity during the lifetime of L and M intermediates, indicating that some of tryptophan residues undergo a change in environment in the vicinity of the retinal chromophore (7). Furthermore, a tryptophan fluorescence quenching study of different perturbations on bR such as deionization and delipidation has shown that different protein conformation changes may occur during the photocycle of bR under these perturbations (8). Recently, it has been reported that the tryptophan emission shows four decay components with lifetimes varying from 100 ps to 2 ns (6), which have been attributed to tryptophan residues in four different environments in bR. The short lived (most quenched) Trp emission is found to have a shorter wavelength, suggesting that it originates from molecules in hydrophobic parts of the protein (6). The variation in the tryptophan emission lifetimes is suggested to result from the variation in the coupling strength of the tryptophan excited state with the retinal chromophore (6). Although these studies provide a better picture of the interaction between the tryptophan residues and the retinal in bR, it is still unclear which specific tryptophan residues are responsible for those interaction discussed above.

Site-specific mutagenesis has been used to examine the possible role of individual amino acids in the structure and function of enzyme protein (9, 10). The effects of systematic substitution of tryptophan residues on the proton pumping efficiency, protein folding, and stability in bR have been reported (11). From the absorption spectral shifts and the measurement of proton pumping efficiency, it is concluded that Trp-86, Trp-182, Trp-189, and possibly Trp-137 interact strongly with the retinal. Low temperature UV/visible (12) and Fourier transform infrared difference spectroscopies (13) have also suggested that Trp-86, Trp-182, and Trp-189 may form part of a retinal binding pocket and

Tatsushi Mogi's present address is Department of Biology, Faculty of Science, University of Tokyo, Hongo, Bunkyo-ku, Tokyo 113, Japan.

0006-3495/92/05/1281/08 $2.00

help restrict the allowed conformation of retinal in this pocket. The effects of Trp-182 and Trp-189 substitution on the photcycle kinetics on the milisecond time scale have been reported (14) and found to be consistent with the conclusion obtained from UV/visible difference spectroscopy (12). Based on spectroscopic studies of bR mutants, it has been proposed that together with Pro-186, Trp-182 and Trp-189 may surround the polyene chain of retinal while Tyr-185 is positioned close to the active site (Schiff base) of bR (15). Very recently, from the UV transient absorption spectroscopic study of tryptophan mutants, Trp-182 has been assigned to be responsible for the UV absorption change at 296 nm during the photocycle, which is believed to result from a charge perturbation imposed by interaction with neighboring charged species (16).

In this study, we have systematically examined the formation and decay kinetics of M intermediate during bR photocycle for nine different tryptophan mutants. It is found that some mutants show very different kinetics as compared with ebR. It is also found that these mutations affect the M formation and decay kinetics differently. It has been explained that mutations in different parts of the protein may affect the protonation and deprotonation channels in different manners. Temperature dependence of M formation kinetics has been performed for several important mutants and ebR in order to understand the origin of the different kinetic behavior, which is discussed in terms of the difference in the energetic and entropic effect on the photocycle of bR for different mutants. The correlation found between the proton pumping activity and the relative amplitudes of the slow M rise for some important mutants has been explained by the parallel cycle model in a simple manner.

MATERIALS AND METHODS

Single substitutions of tryptophan residues by phenylalanine or cystine were carried out by the cassette replacement mutagenesis (11, 17a,b). The details of the cloning and expression of wild-type bR (ebR) and mutants have been reported previously (11, 17a,b, 18). The proteins were reconstituted in vesicles with the polar lipid from *H. Halobium,* using a protein/lipid weight ratio of 1:1 (19), and buffered at 6 (sodium phosphate).

The photocycle transient absorption measurement has been described previously (20). The photolysis of bR was accomplished with 580-nm pulses from an N_2-pumped dye laser pulse and had an energy of ~50 μJ with a temporal width of 0.5 ns and was collimated and focused to an ~2-mm spot size. The 405-nm probe light was the output of a 100-W Hg arc lamp (Pek Labs 401; Sunnyvale, CA) passed through filters and focused into a 0.25-m monochromator (Jarrel-Ash 82-410; Waltham, MA). The wavelength-selected probe beam was detected by a photomultiplier tube (RCA 1P28A, Lancaster, PA) and recorded with a transient digitizer (Biomation 8100 waveform recorder; Princeton Applied Research Corp., Princeton, NJ), which was interfaced to the PC computer. The signals were averaged for 1,000–2,000 shots and then converted to transient absorption in optical density. Sample temperatures were regulated using a water bath (Neslab RTE100D; Dublin, CA) and measured with a digital thermometer (Fisher Scientific NBS LCD; Pittsburgh, PA) using a 3-mm probe (YSI402).

RESULTS AND DISCUSSION

(a) Effects of mutation on the kinetics of deprotonation and reprotonation processes

Table 1 shows the rise kinetics of M intermediates monitored at 405 nm in the photocycle of ebR and the tryptophan mutants. The kinetics are fitted as either biexponential or single-exponential form according to χ^2 judgement. Comparing with ebR, most of the mutants show more or less different kinetic behavior in terms of either rate constants or relative amplitudes for fast and slow phase of the kinetics. Of all the mutants, W10F, W12F, W80F, and possibly W138F mutants seem to be least affected by mutation, indicating that Trp-10, Trp-12, Trp-80, and Trp-138 residues are not important to the deprotonation process of the bR photocycle. Previously (11), it had been found that substitutions of Trp-10 and Trp-12 did not cause any significant change in the regeneration rate and in the absorption maxima of the chromophore, which is consistent with the model in which Trp-10 and Trp-12 are located close to the extracellular side of the putative helix A. The substitutions of Trp-80 and Trp-138 were also found to have only minor effects on the proton pumping activity, the regeneration rate of the chromophore and other protein properties (11). Our results of the M-formation kinetics

TABLE 1 Rate constants for the formation of M intermediate for ebR and tryptophan mutants at pH 6.0 and 22°C

Sample	Rate constants (10^4 s^{-1})		Amplitudes (%)		τ_{ave}* (μs)
	k_{fast}	k_{slow}	A_{fast}	A_{slow}	
ebR	10.2	1.4	18	82	60
W10F	10.3	2.5	30	70	31
W12F	12.0	2.7	20	80	31
W80F	10.8	2.2	24	76	37
W86F	26.9	2.9	84	16	8.6
W137C	9.2	4.1	22	78	21
W138C	11.2	2.5	35	65	29
W138F	8.2	2.1	51	49	30
W182F	4.0	0.4	17	83	212
W189F	9.3	2.4	64	36	22

*Average formation time τ_{ave} is calculated according to equation: $\tau_{ave} = A_{fast}/k_{fast} + A_{slow}/k_{slow}$.

for these mutants agree with these observations, indicating that the replacement of these tryptophan residues has the insignificant effects on the interaction between these residues and the membrane-embedded polypeptide chain.

From Table 1, it is more interesting to note that the replacement of Trp-86, Trp-182, Trp-189, and possibly Trp-137 shows the substantial effects on the M-formation kinetics as compared with that of ebR. Much faster rate of M rise is observed for W86F mutant than that of ebR. In contrast to the W86F mutant, the W182F mutant shows a very slow M rise kinetics as compared with that of ebR. Average formation rates are calculated for ebR and all the tryptophan mutants as shown in Table 1. The rate is 7 times faster for the W86F mutant and 3.5 times slower for the W182F mutant than the average rate constant of ebR. The M rise kinetics of W137C and W189F are also faster than that of ebR but to a lesser degree with respect to that of W86F.

To visualize and emphasize the difference in the kinetics, Fig. 1 shows the formation kinetics of the M intermediate monitored at 405 nm for ebR, W86F, and W182F mutants. The results shown in Fig. 1 can be interpreted as following. Because the Trp-86 is in proximity of the Asp-85 in primary protein sequence, the decrease in its side-chain volume and/or the increase in its hydrophobicity could change its intramolecular interaction with the Asp-85 residue to increase the deprotonation rate of the Schiff base because Asp-85 has been believed to be directly involved in proton translocation (21), especially as a possible internal proton acceptor from the Schiff base (22). Therefore, the presence of Trp-86 in the bR may restrict the conformation of Asp-85 in such a fashion that the process of proton transfer to Asp-85 from the Schiff base is slowed down. From FTIR difference spectroscopy (13), it has been reported that Trp-86 undergoes a structural alteration during the bR → K photoreaction, suggesting that Trp-86 interacts with residues Asp-85, Tyr-185, and Trp-189. Our results agree with this observation because the replacement of Trp-189 also increases the rate constant of the deprotonation process of the Schiff base, indicating that Trp-86 and Trp-189 have a similar effect on the photocycle kinetics. According to the structure model proposed by Mathies et al. (23), both Trp-86 and Trp-189 are positioned below the center of the polyene chain of the chromophore. However, it is still not clear whether direct interaction between residues or secondary effects due to structural changes upon mutation are responsible for these observed effects.

The mutation of Trp-182 has a different effect on the deprotonation step of bR photocycle because of its substantially reduced M rise rate constant, which is in contrast to the increased rate constants observed for Trp-86 and Trp-189. Mogi et al. have reported that the substitutions of Trp-182 and Trp-189 with Phe change the properties of bR (11). Based on the FTIR study (13), it has been proposed that Trp-182 and Trp-189 are located within the retinal binding pocket to directly or indirectly influence the configuration of retinal. However, the different kinetic effects are observed for

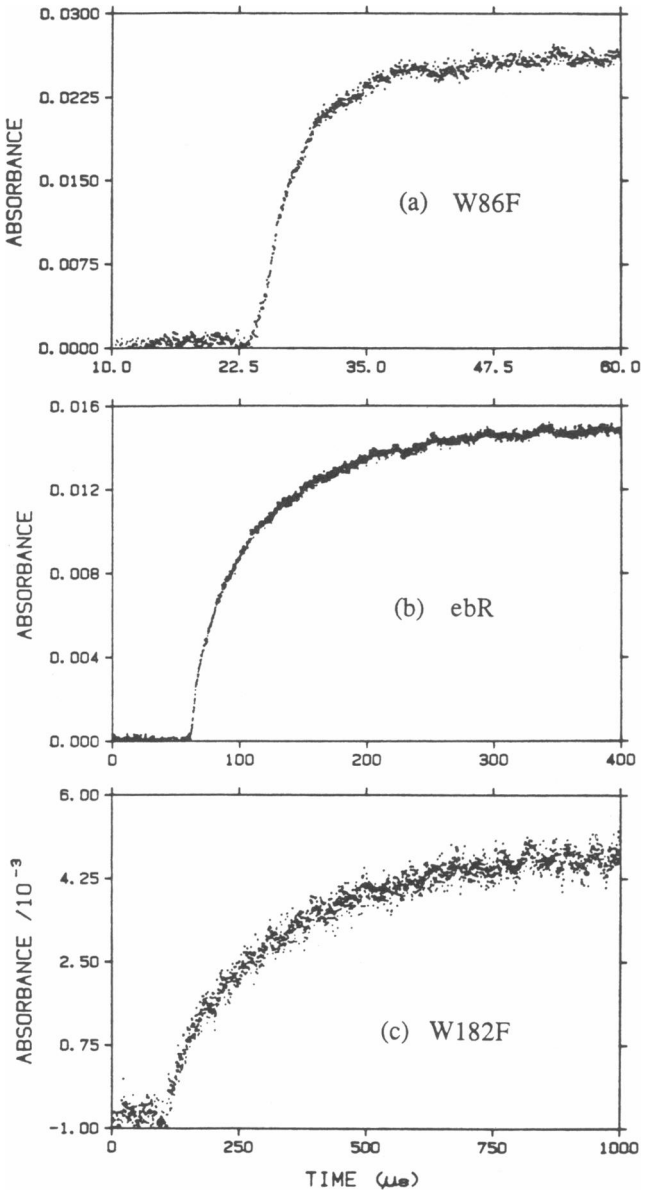

FIGURE 1 Formation kinetics of M intermediate in the photocycle of ebR and selected tryptophan mutants. Samples were photolyzed at 580 nm and the signal was monitored at 405 nm. (*a*) W86F; (*b*) ebR; (*c*) W182F.

Trp-182 and Trp-189 mutants, suggesting these two residues may have a different kind of effect on the interaction between the two groups and the retinal chromophore or other protein residues. According to Mathies et al. (23), Trp-182 probably prevents the motion of the chromophore in the vertical direction while Trp-189 probably restrains the motion of the β-ionone ring of the chromophore. Recently, it has been found that during the formation time of the M intermediate, there is a charge interaction between Trp-182 and a neighboring charged species (16). Although no certain assignment has been made for this charged spcies, some possible candidates in the retinal binding pocket are discussed (16). Therefore, we suggest that a possible charge coupling among the Trp-182, the Schiff base, and the other charged residues, which are believed to be involved in the proton pump, may account for the observed unique kinetic behavior of the Trp-182 mutant.

Table 2 summarizes the decay kinetic parameters of the M intermediate in the photocycle of ebR and the tryptophan mutants, and Fig. 2 shows the decay kinetics of selected tryptophan mutants in comparison with Fig. 1. It seems that the mutation of tryptophan residues in bR does not affect the reprotonation step as much as the deprotonation step, especially for Try-86, Trp-182, Trp-137, and Trp-189 mutants. The calculated average decay times for all the mutants are found to be reasonably close to the value observed for ebR as shown in Table 2. This result can be explained by proposing that some tryptophans such as Trp-86, Trp-182, etc. are located in the part of the deprotonation channel of the protein whose conformation changes control the rate of the deprotonation of PSB so that the replacement of these residues only affects the rate of the deprotonation but not the reprotonation process.

TABLE 2 Rate constants for the decay of M intermediate for ebR and tryptophan mutants at pH 6.0 and 22°C

Sample	Rate constants (10^2 s^{-1})		Amplitudes (%)		τ_{ave}* (ms)
	k_{fast}	k_{slow}	A_{fast}	A_{slow}	
ebR	7.1	1.2	28	72	6.4
W10F	4.1	0.74	29	71	10.3
W12F		1.34	single exp		7.5
W80F		1.40	single exp		7.1
W86F	3.0	0.81	44	56	8.4
W137C	7.2	0.80	15	85	10.8
W138C	NA				
W138F		1.30	single exp		7.7
W182F		1.80	single exp		5.6
W189F	7.1	1.20	20	80	6.4

Average decay time τ_{ave} is calculated according to equation: $\tau_{ave} = A_{fast}/k_{fast} + A_{slow}/k_{slow}$.

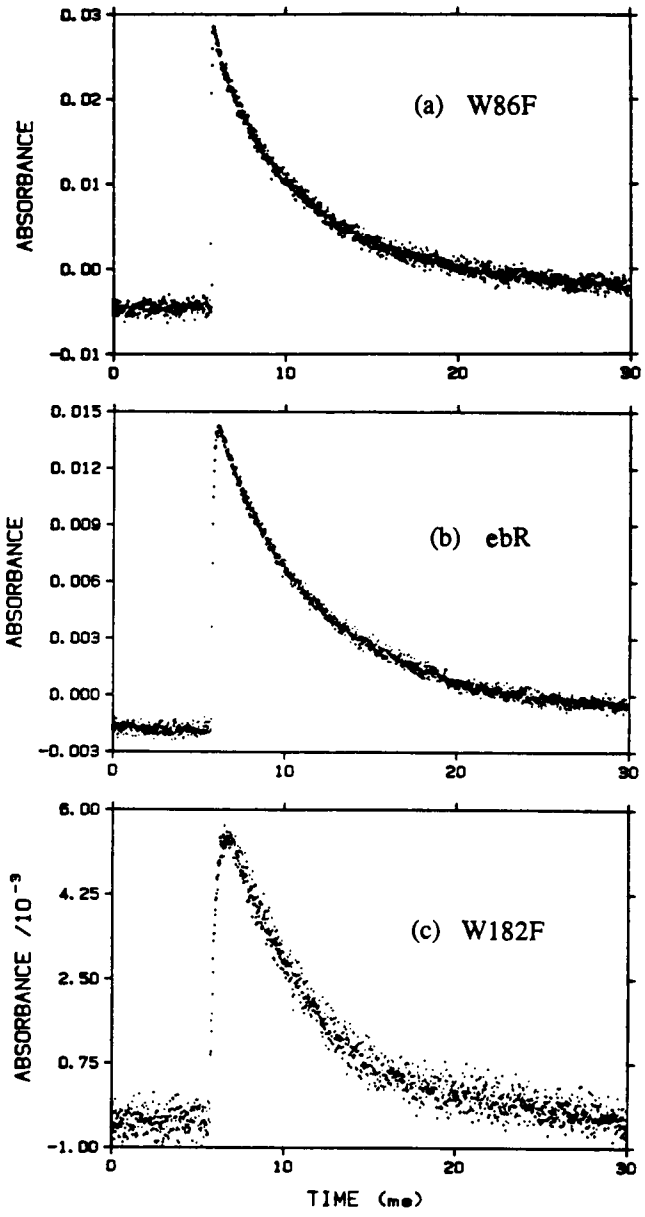

FIGURE 2 Decay kinetics of M intermediate in the photocycle of ebR and selected tryptophan mutants. Samples were photolyzed at 580 nm and the signal was monitored at 405 nm. (*a*) W86F; (*b*) ebR; (*c*) W182F.

(*b*) Effects of mutation on the temperature dependence of the deprotonation process

Temperature dependence studies of the rate of M rise enable one to estimate the activation energy and entropy for the deprotonation process of the Schiff base. To find out whether different kinetics of M rise observed for

different mutants are due to energetic or entropic effects, we carried out the measurement of the rate constant of M rise at several different temperatures. Some representatives of Arrhenius plots are shown in Fig. 3 and the activation parameters are summarized in Table 3. The Arrhenius plots shown in Fig. 3 for ebR and W182F mutant are drawn for the slow component (having more than 80% of the total amplitude in both samples) of the M-formation kinetics while the plot for the W86F mutant is for the fast component (84%). The Arrhenius energy and entropy of activation for the W86F mutant is found to be only 17 kJ/mol and −92 J/K-mol as compared with 80 kJ/mol and 95 J/K-mol of ebR. If the slow component for W86F is used to make the Arrhenius plot, the derived activation parameters (not shown in Fig. 3) are 36 kJ/mol and −35 J/K-mol for the activation energy and entropy, respectively. Although the values are higher than those obtained for the fast process (main component), they are still substantially smaller than the values for ebR so that the same conclusion can be reached. In contrast to the W86F mutant, W182F has slightly higher values of 95 kJ/mol and 137 J/K-mol for the activation energy and entropy, respectively, than those of ebR. Furthermore, the preexponential factors (f) are also calculated and can be found in Table 3. It can be seen that the f value is much smaller for the W86F mutant and slightly larger for the W182F mutant than that of ebR, which suggests that the entropy of activation contributes more to the rate of deprotonation in the W86F mutant, but the energy of activation contributes more in the W182F mutant, which can be rationalized from the Wynne-Jones and Eyring equation. Therefore, different energetic and entropic effects for these two mutants may well explain their drastically different influence on the M rise kinetics, implying that the replacement of these two residues leads to different types of protein conformational changes.

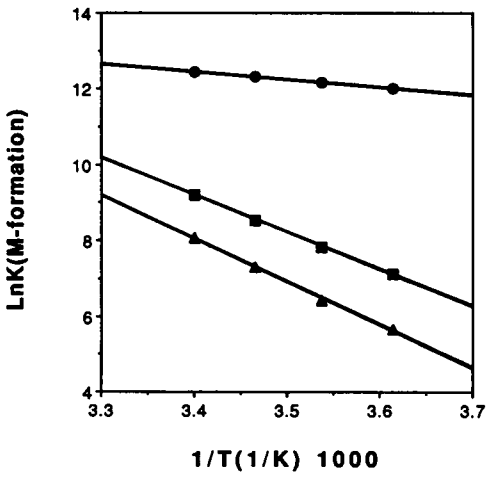

FIGURE 3 Arrhenius plots of the M formation in the photocycle of ebR, W86F, and W182F mutants. The derived activation parameters are summarized in Table 2. (■) ebR; (●) W86F; (▲) W182F.

TABLE 3 **Activation parameters of the M-formation for ebR and selected tryptophan mutants at pH 6.0 and 25°C**

Sample	E_a	$\Delta H_a^{\ddagger}$	$\Delta S_a^{\ddagger}$	$\Delta G_a^{\ddagger}$	f*
	kJ/mol	kJ/mol	J/K-mol	kJ/mol	1/s
ebR	80.0	77.5	95	49.2	9.5×10^{17}
W86F	17.0	14.5	−92	41.9	2.4×10^{8}
W182F	95.0	92.5	137	51.7	1.2×10^{20}

*f values (frequency factor) are calculated from equation: $k = f \exp(-E_a/RT)$; $^{\ddagger}\Delta H_a$, ΔS_a, and ΔG_a are estimated from the Wynne-Jones and Eyring equation: $k = kT/h \exp(\Delta S_a/R - \Delta H_a/RT) = kT/h \exp(-\Delta G_a/RT)$.

The activation energy for the deprotonation of the Schiff base in the W86F mutant is 17 kJ/mol, which is close to the value of 13 kJ/mol for diffusion-controled proton transfer reaction in water (24). In the W86F mutant, the hydrogen-bonding groups present in the side chain of Trp-86 is replaced by a phenylalanine which has a non-hydrogen-bonding group in the side chain. The fact that ebR has a higher activation energy (80 kJ/mol) than the W86F mutant (17 kJ/mol) suggests that the formation of the hydrogen-bonding network in ebR through an interaction between the Trp-86 residue and other amino acid side chains and H_2O molecules gives rise to an activated protein conformation that renders a higher energy and entropy of activation for the deprotonation process in ebR. Upon mutation of Trp-86, the H-bond is no longer present and a more open structure leading to a diffusion-controled process of deprotonation, probably involving H_2O molecules, becomes operative. Based on Henderson's structure (25), Mathies et al. have performed the energy minimization for the bR structure (23). They found that the strain caused by the contact between the retinal chromophore and Trp-86 is partly relieved by distorting the retinal chain along the C_{13}=C_{14} and C=N bonds and slightly lowering the indole ring. In this energy-minimized structure of bR, the Asp-212 is hydrogen bonded to the N → H group of the Schiff base and then interacts with the indole nitrogen of Trp-86 and the hydroxyl group of Tyr-185. Together with the Asp-85 and Arg-82, Asp-212, Trp-86, and Tyr-185 form the counterion environment for the Schiff base (23). Therefore, we may conclude from our results that the Trp-86 is involved in forming the hydrogen-bonding network with Asp-212 and possi-

bly the H_2O molecules. The possible involvement of H_2O molecules is not indicated by Mathies' structure model.

(c) Effects of mutation on the correlation of proton pumping activity with different kinetic parameters

In Table 4, a comparison is given of the kinetic results of the M-formation and decay of mutants that have the largest perturbation effects on the kinetics with their relative initial proton-pumping activity (11). It seems that there is a direct correlation between the relative amplitudes of the slow rise component and the proton pumping activity but not with the formation rate constants (Table 4). A correlation of the microsecond photocurrent component with the L → M optical transition was proposed by Liu for oriented purple membrane film (26). As shown in Table 4, the proton pumping activity decreases as the relative amplitude of the slow rise component decreases for the molecules in the order of ebR, W182F, W138F, W189F, and W86F. As discussed below, these results can best be described in terms of the heterogeneity model that proposes the presence of two types of bR with two photocycles (27–32), rather than the model that proposes the presence of a pH-dependent reverse reaction (33–36) to account for the two observed components of M rise and decay of pmbR.

The observation that at a constant pH of 6.0, the relative amplitudes, and not the rate constants, are correlated with the mutation type perturbation, cannot be described in a simple manner by a pH-dependent (N → M → L) reverse reaction model (33–36). In this model, the values of k_{slow} and k_{fast} are sensitive to the pH and determine the apparent values of the amplitudes. Since the pH is constant, mutation perturbs the photocycle by changing its rate constants, and thus one would expect that this perturbation would change the relative amplitudes in accordance with the corresponding changes in the rate constants. Upon examining the kinetic parameters of the mutants in Table 4, we observe no correlation between the values of k and those of the amplitudes for the rise or the decay of M at constant pH. Of course, the dependence could be of such complex nature that it, somehow, washes out.

The heterogeneity model, however, can in a simple and direct manner explain the observed results. In the heterogeneity model (27–32), the presence of two or more bR results from the pocket environment that is determined by an acid-base equilibrium involving an amino acid with a pKa ~9 (27); one of the bRs has a slow formation rate and the other has a fast one. Due to the difference in the environment of the protonated Schiff base in the two bR molecules, the reaction potential surface is such that only allows the one with the slow rise to pump, or to initiate the pumping of the dissociated proton to the outside surface while the fast one does not produce external protons. Since the two forms of bR are in acid-base equilibrium (27), the relative amplitudes of the fast and slow components in both the rise and decay of M reflect the relative mole fractions of the two forms in pmbR only if the rate of equilibration between the two forms is slower than the rate of M rise and decay (37). The fact that the relative amplitudes of the fast and slow components in the M decay are different from those of the M formation in pmbR; ebR or its mutants suggest that the rate of equilibration between the two forms takes place on a time scale that is comparable to the M decay (37).

The authors would like to thank a conscientious reviewer who directed our attention to the correlation between the proton pumping efficiency and the slow rise amplitudes of M intermediates. We also thank Hyun-Jin Hwang for helping to install the new data acquisition system and developing the programs for data analysis.

The work at UCLA was supported by the Department of Energy, Office of Basic Energy Science, under grant DE-FG03-88ER13828. The work of MIT was supported by National Institutes of Health grant GM-28289-09 and an Office of Naval Research grant N00014-82-K-0668.

TABLE 4 Comparison of the formation and decay kinetics of M intermediate with the proton pumping activity for ebR and selected tryptophan mutants

Sample	Rise rate constants (10^4 s^{-1})		Decay rate constants (10^2 s^{-1})	Amplitudes for decay (%)	Amplitudes for rise (%)		Pumping activity*
	k_{fast}	k_{slow}	k_{slow}	A_{slow}	A_{fast}	A_{slow}	
ebR	10.2	1.4	1.2	0.72	18	82	1.0
W182F	4.0	0.4	1.8	1.0	17	83	0.76
W138F	8.2	2.1	1.3	1.0	51	49	0.56
W189F	9.3	2.4	1.2	0.8	64	36	0.50
W86F	26.9	2.9	0.8	0.56	84	16	0.26

*Reference 11. The control activity of proton pumping for ebR is 3.4 H^+/bR/s at pH 7.

Received for publication 20 September 1991 and in final form 13 January 1992.

REFERENCES

1. Stoeckenius, W., and R. A. Bogomolni. 1982. Bacteriorhodopsin and related pigments of halobacteria. *Annu. Rev. Biochem.* 51:587–616.
2. Khorana, H. G., G. E. Eerber, W. C. Herlihy, C. P. Gray, R. J. Anderegg, K. Nihei, and K. Biemann. 1979. Amino acid sequence of bacteriorhodopsin. *Proc. Natl. Acad. Sci. USA.* 76:5046–5050.
3. Arseniev, A. S., A. B. Kuryatov, V. I. Tsetlin, V. F. Bystrov, V. T. Ivanov, and Yu. A. Ovchinnikov. 1987. ^{19}F NMR study of 5-fluorotryptophan-labeled bacteriorhodopsin. *FEBS Lett.* 213: 283–288.
4. Palmer, P. L., and W. V. Sherman. 1985. Alkaline quenching of bacteriorhodopsin tryptophanyl fluorescence: evidence for aqueous accessibility or a hydrogen-bonded chain. *Photochem. Photobiol.* 42:541–547.
5. Sherman, W. V. 1982. Time-resolved fluorometry of bacteriorhodopsin. *Photochem. Photobiol.* 36:463–469.
6. Jang, D.-J., T. C. Corcoran, and M. A. El-Sayed. 1988. Effect of metal cations, retinal, and the photocycle on the tryptophan emission in bacteriorhodopsin. *Photochem. Photobiol.* 48:209–217.
7. Fukumoto, J. M., W. D. Hopewell, B. Karvaly, and M. A. El-Sayed. 1981. Time-resolved protein fluorescence studies of intermediates in the photochemical cycle of bacteriorhodopsin. *Proc. Natl. Acad. Sci. USA.* 78:252–255.
8. Jang. D.-J., and M. A. El-Sayed. 1989. Tryptophan fluorescence quenching as a monitor for the protein conformation changes occurring during the photocycle of bacteriorhodopsin under different perturbations. *Proc. Natl. Acad. Sci. USA.* 86:5815–5819.
9. Ackers, G. K., and R. F. Smith. 1985. Effects of site-specific amino acid modification on protein interactions and biological function. *Annu. Rev. Biochem.* 54:597–629.
10. Knowles, J. R. 1987. Thinking with enzymes: what are we learning? *Science (Wash. DC).* 236:1252–1258.
11. Mogi, T., T. Marti, and H. G. Khorana. 1989. Structure-function studies on bacteriorhodopsin. IX. Substitutions of tryptophan residues affect protein-retinal interaction in bacteriorhodopsin. *J. Biol. Chem.* 264:14197–14201.
12. Ahl, P. L., L. J. Stern, D. During, T. Mogi, H. G. Khorana, and K. J. Rothschild. 1988. Effects of amino acid substitutions in the F helix of bacteriorhodopsin. *J. Biol. Chem.* 263:13594–13601.
13. Rothschild, K. J., D. Gray, T. Mogi, T. Marti, M. S. Braiman, L. J. Stern, and H. G. Khorana. 1989. Vibrational spectroscopy of bacteriorhodopsin mutants. Chromophore isomerization perturbs tryptophan-86. *Biochemistry.* 28:7052–7059.
14. Ahl, P. L., L. J. Stern, T. Mogi, H. G. Khorana, and K. J. Rothschild. 1989. Substitution of amino acids in helix F of bacteriorhodopsin: effects on the photochemical cycle. *Biochemistry.* 28:10028–10034.
15. Rothschild, K. J., M. S. Braiman, T. Mogi, L. J. Stern, and H. G. Khorana. 1989. Conserved amino acids in F-helix of bacteriorhodopsin form part of a retinal binding pocket. *FEBS Lett.* 250:448–452.
16. Wu, S., D.-J. Jang, M. A. El-Sayed, T. Marti, T. Mogi, and H. G. Khorana. 1991. The use of tryptophan mutants in identifying the 296 nm transient absorbing species during the photocycle of bacteriorhodopsin. *FEBS Lett.* 284:9–14.

17a. Otto, H., T. Marti, M. Holz, T. Mogi, M. Lindau, H. G. Khorana, and M. P. Heyn. 1989. Aspartic acid-96 is the iternal proton donor in the reprotonation of the Schiff base of bacteriorhodopsin. *Proc. Natl. Acad. Sci. USA.* 86:9228–9232.

17b. Otto, H., T. Marti, M. Holz, T. Mongi, L. J. Stern, F. Engel, H. G. Khorana, and M. P. Heyn. 1990. Substitution of amino acids Asp-85, Asp-212 and Arg-82 in bacteriorhodopsin affects the proton release phase of the pump and the pK of the Schiff base. *Proc. Natl. Acad. Sci. USA.* 87:1018–1022.

18. Hackett, N. R., L. J. Stern, B. H. Chao, K. A. Kronis, and H. G. Khorana. 1987. Structure-function studies on bacteriorhodopsin. V. Effects of amino acid substitutions in the putative helix F. *J. Biol. Chem.* 262:9277–9284.
19. Popot, J. L., S. E. Gerchman, and D. M. Engelman. 1987. Refolding of bacteriorhodopsin in lipid bilayers.A thermodynamically controlled two-stage process. *J. Mol. Biol.* 198:655–676.
20. Wu, S., E. S. Award, and M. A. El-Sayed. 1991. Circular dichroism and photocycle kinetics of partially detergent solubilized and partially retinal regenerated bacteriorhodopsin. *Biophys. J.* 59:70–75.
21. Mogi, T., L. J. Stern, T. Marti, B. H. Chao, and H. G. Khorana. 1988. Aspartic acid substitutions affect proton translocation by bacteriorhodopsin. *Proc. Natl. Acad. Sci. USA.* 85:4148–4152.
22. Braiman, M. S., T. Mogi, T. Marti, L. J. Stern, H. G. Khorana, and K. J. Rothschild. 1988. Vibrational spectroscopy of bacteriorhodopsin mutants. Light-driven proton transport involves protonation changes of Aspartic acid residues 85, 96, and 212. *Biochemistry.* 27:8516–8520.
23. Mathies, R. A., S. W. Lin, J. B. Ames, and W. T. Pollard. 1991. From femtoseconds to biology: mechanism of bacteriorhodopsin's light-driven proton pump. *Annu. Rev. Biophys. Biophys. Chem.* 20:491–518.
24. Eigen, M., and L. DeMaeyer. 1955. Untersuchungen uber die kinetik der neutralization. 1.*Z. Elektrochem.* 59:986–993.
25. Henderson, R., J. M. Baldwin, T. A. Ceska, F. Zemlin, E. Beckmann, and K. H. Downing. 1990. Model for the structure of bacteriorhodopsin based on high-resolution electron cryomicroscopy. *J. Mol. Biol.* 213:899–929.
26. Liu, S. Y. 1990. Light-induced currents from oriented purple membrane. I. Correlation of the microsecond component (B2) with the L-M photocycle transition. *Biophys. J.* 57:943–950.
27. Hanamoto, J., P. Dupuis, and M. A. El-Sayed. 1984. On the protein (tyrosine)-chromophore (protonated Schiff base) coupling in bacteriorhodopsin. *Proc. Natl. Acad. Sci. USA.* 81:7083–7087.
28. Dancshazy, Zs., R. Govindjee, and T. G. Ebrey. 1988. Independent photocycles of the spectrally distinct forms of bacteriorhodopsin. *Proc. Natl. Acad. Sci. USA.* 85:6358–6361.
29. Balashov, S. P., N. V. Karneyeva, E. S. Imasheva, and F. F. Litvin. 1986. Two forms of *trans*-bacteriorhodopsin and their photoreactions at 77 K. *Biophysics (Engl. Transl.).* 31:1070–1073.
30. Diller, R., and M. Stockburger. 1988. Kinetics resonance Raman studies reveal different conformational states of bacteriorhodopsin. *Biochemistry.* 27:7641–7651.
31. Bitting, H. C. Jr., D.-J. Jang, and M. A. El-Sayed. 1990. On the multiple cycles of bacteriorhodopsin at high pH. *Photochem. Photobiol.* 51:593–598.

32. Li, Q.-Q., R. Govindjee, and T. G. Ebrey. 1984. A correlation between proton pumping and the bacteriorhodopsin photocycle. *Proc. Natl. Acad. Sci. USA.* 81:7079–7082.

33. Varo, G., and J. K. Lanyi. 1990. Pathways of the rise and decay of the M photointermediate(s) of bacteriorhodopsin. *Biochemistry.* 29:2241–2250.

34. Varo, G., A. Duschl, and J. K. Lanyi. 1990. Interconversions of the M, N, and O intermediates in the bacteriorhodopsin photocycle. *Biochemistry.* 29:3798–3804.

35. Fodor, S. P. A., J. B. Ames, R. Gebhard, E. M. M. van den Berg, W. Stoeckenius, J. Lugtenburg, and R. A. Mathies. 1988. Chromophore structure in bacteriorhodopsin's N intermediate: implications for the proton-pumping mechanism. *Biochemistry.* 27:7097–7101.

36. Ames, J. B., and R. A. Mathies. 1990. The role of back-reactions and proton uptake during the N → O transition in bacteriorhodopsin's photocycle: a kinetic resonance Raman study. *Biochemistry.* 29:7181–7190.

37. Lin, G. C., E. S. Award, and M. A. El-Sayed. 1991. Temperature and pH dependence of the deprotonation step L550 → M412 in the bacteriorhodopsin photocycle. *J. Phys. Chem.* 95:10442–10447.